Kidney International, Vol. 60 (2001), pp. 597–606

Renal fibroblast-like cells in Goodpasture syndrome rats

Hirokazu Okada, Tsutomu Inoue, Yoshihiko Kanno, Tatsuya Kobayashi, Shinichi Ban, Raghurum Kalluri, and Hiromichi Suzuki

Departments of Nephrology and Pathology, Saitama Medical College, Saitama, Japan, and Nephrology Division, Beth Israel Deaconess Medical Center, Harvard Medical School, Boston, Massachusetts, USA

Renal fibroblast-like cells in Goodpasture syndrome rats.

Background. The extent of renal fibrosis is the best predictor for functional outcomes in a variety of progressive renal diseases. Interstitial fibroblast-like cells (FbLCs) are presumably involved in the fibrotic process. However, such FbLCs have never been well characterized in the kidney.

Methods. We characterized renal FbLCs in the nephritic kidney (in which the number of FbLCs and extracellular matrix accumulation were significantly increased) with regards to their expression of phenotypic and functional markers using day 49 Goodpasture syndrome (GPS) rats.

Results. Within the renal cortical interstitium, there were a number of α-smooth muscle actin$^+$ (α-SMA$^+$) FbLCs, negative for vimentin (VIM) and transforming growth factor-β1, and not equipped with well-developed rough endoplasmic reticulum and actin-stress fibers. All of these findings were incompatible with the typical features of granulation tissue α-SMA$^+$ myofibroblasts. On the other hand, FbLCs negative for α-SMA and VIM produced α1(I) procollagen in the nephritic kidney.

Conclusion. A number of FbLC populations reside within the cortical interstitium of the kidney in GPS rats, each of which is likely to have developed independently in response to the local conditions of the nephritic kidney, contributing to renal fibrogenesis. Further studies are needed to clarify the key type of FbLC that orchestrates other members to produce renal fibrosis.

Renal fibrosis is a final common pathway through which most chronic renal diseases progress to end-stage renal failure [1–4]. It has long been noted in the various types of glomerular disease that the degree of renal interstitial alteration correlated better than glomerular damage itself with renal function at the time of biopsy and with the prognosis of the disease [5, 6]. Interstitial alterations in the nephritic kidney consist of infiltrating immune cells, atrophic tubules, and fibrosis. Fibroblasts (Fbs) are thought to be stimulated by infiltrating immune cells, activated resident renal cells, and Fbs themselves to produce extracellular matrix (ECM) molecules and to populate such interstitial areas in parallel with the atrophy and the loss of normal integrity to generate a classical form of fibrosis [1–3].

In contrast to the well-characterized cellular components within the interstitium of healthy kidneys, for example, Fbs and lipid-laden interstitial cells (type I interstitial cells), macrophages (type II interstitial cells), and dendritic cells [7], these components in the nephritic kidney still require further morphological and functional investigation. Fibroblasts are not homogeneous and consist of a variety of functionally different interstitial cells called fibroblast-like cells (FbLCs) in a given interstitium [8, 9]. Especially in a diseased interstitium, Fbs are thought to be highly heterogeneous, but this remains to be characterized. Among them, only granulation tissue Fbs termed myofibroblasts (myoFbs) in the skin have been intensively investigated because of their readily available muscle-related phenotypic markers, for example, α-smooth muscle actin (α-SMA), vimentin (VIM), desmin (DSM), and myosin heavy chain (MYS) [9, 10]. Most investigators interested in organ fibrosis have focused on α-SMA$^+$ FbLCs as presumed myoFbs in any given organ, and they seem to pay little attention to the heterogeneity of α-SMA$^+$ FbLCs within different organs. However, even the origin of α-SMA$^+$ FbLCs has remained largely undetermined in most organs, despite the considerable number of proposed candidates, for example, Fbs, vascular smooth muscle cells, vascular pericytes, tubular epithelium, endothelial cells, monocytes, etc. [9–17]. In addition, the exact contribution of α-SMA$^+$ FbLCs to fibrogenesis still requires confirmation, especially within the kidney [1–4, 13, 18–21]. In this study, in order to characterize renal FbLCs within a diseased interstitium, we determined the in vivo phenotype and cell biology of FbLCs in the nephritic kidney of Goodpasture syndrome (GPS) rats.

Key words: renal fibrosis, fibroblasts, myofibroblasts, α-smooth muscle actin, vimentin, α1(I)procollagen.

Received for publication September 6, 2000
and in revised form February 21, 2001
Accepted for publication February 23, 2001

METHODS

Animal model and tissue sampling

Goodpasture syndrome generated in rats by our method is essentially identical to the disease in human; the prepa-

ration and characterization of GPS rats have been previously reported in detail [22, 23]. Wistar rats subcutaneously injected with adjuvant alone were used as the controls. Five rats were sacrificed at each time point on day 21, 28, 35, 42, 49, and 56, and kidney tissues were collected from each rat. One whole kidney from each rat was used for RNA extraction. Tissues of the other kidney were fixed in 4% phosphate saline-buffered paraformaldehyde overnight. One part of each tissue specimen was processed into paraffin blocks for histopathology and immunohistochemistry analyses. Another part of the tissue samples was rinsed in serial concentrations of sucrose and then snap frozen for immunofluorescence and in situ hybridization (ISH). The rest of the fixed tissue was processed for IEM as described later.

Immunohistochemistry and morphometric analysis

Sections were cut 4 μm in thickness from the paraffin blocks and processed for hematoxylin and eosin (HE) staining and the indirect immunoperoxidase method described in detail previously [22, 23]. Mouse anti-α-SMA (1:500; Sigma, St. Louis, MO, USA), anti-VIM (1:500; Dako Japan, Kyoto, Japan), anti-rat monocytes (ED-1; 1:200; Chemicon International, Temecula, CA, USA), and rabbit anti-rat tail Col I (1:400) [14] were applied as primary antibodies. Twenty cortical fields at ×100 magnification were assessed quantitatively in each immunostained section using a color image computer analyzer (Mac SCOPE, version 2.5; Mitani Corp., Hukui, Japan). All glomeruli and vessels were subtracted from a given field, yielding a target area of tubulointerstitium. Interstitial ED-1$^+$ monocyte infiltration was expressed as the mean cell number in the tubulointerstitium. Interstitial α-SMA$^+$ FbLCs and tubulointerstitial VIM$^+$ cells, and interstitial Col I accumulation were expressed as the percentage of positive area in the tubulointerstitium.

Dual immunofluorescence (DIF) was performed on 4 μm cryostat sections. The primary antibodies employed were as follows: FITC-conjugated mouse anti-α-SMA (1:500; Sigma), anti-VIM (1:500), anti-MYS (1:100; Santa Cruz Biotechnology, Santa Cruz, CA, USA), rabbit anti-DSM (1:200, Monosan, Uden, Netherlands), and anti-ecto-5′-nucleotidase (5′-NT; a marker for type I interstitial cells; 1:1000, generous gift from B. Kaissling, Basel University, Basel, Switzerland [7]). To label cells producing tissue inhibitor of metalloproteinase-1 (TIMP-1) and proliferating cells positive for proliferating cell nuclear antigen (PCNA), mouse anti–TIMP-1 (1:100; Oncogene Research Products, Cambridge, MA, USA) and Phycoerythrin-conjugated mouse anti-PCNA (1:100; Antigenix America, Franklin Square, NY, USA) were used, respectively. To label cells secreting transforming growth factor-β1 (TGF-β1) and platelet-derived growth factor-B (PDGF-B) chain, rabbit anti-TGF-β1 (LC1-30; 1:500, generous gift from J. Kopp, National Institutes of Health, Bethesda, MD, USA) and mouse anti-PDGF-B chain (PGF-007; 1:100, generous gift from Mochida Pharmaceutical, Tokyo, Japan) were used, respectively. The secondary antibodies employed were as follows: Rhodamine-conjugated anti-rabbit IgG and anti-mouse IgG (1:500; Chemicon International) and FITC-conjugated anti-rabbit IgG and anti-mouse IgG (1:500; American Qualex, San Clemente, CA, USA). These dual-stained sections were analyzed with a confocal microscope (MRC600; Bio-Rad Laboratories, Hercules, CA, USA). All of the secondary antibodies had been isolated by immunoaffinity chromatography and absorbed for dual labeling. Control measures included omitting the primary antibody and substituting the primary antibody with normal IgG from the same animal.

Immunoelectron microscopy

A postembedding immunogold technique was used to demonstrate the ultrastructural features of α-SMA$^+$ FbLCs. After overnight fixation with 4% paraformaldehyde, the tissues were dehydrated in 70% ethanol at 4°C for 10 minutes, 95% ethanol at room temperature (RT) for 10 minutes, and 100% ethanol at RT for 15 minutes, followed by three repetitions of the final step. The tissue was then embedded in LR White resin (London Resin, Berkshire, UK). Ultrathin sections were captured on uncoated nickel grids and then mounted consecutively on top of a drop of the following reagents: (*1*) 0.01 mol/L phosphate-buffered saline (PBS; pH 7.4) six times for one minute at 4°C; (*2*) 5% bovine serum albumin in 0.01 mol/L PBS (pH 7.4) for 15 minutes at RT; (*3*) mouse anti-α-SMA (1:500) overnight at 4°C; (*4*) same as step 1; (*5*) gold-labeled anti-mouse IgG (AutoProbe; diameter 15 nm; Amersham Pharmacia Biotech, Uppsala, Sweden) for 30 minutes at RT; (*6*) same as step 1; (*7*) distilled water six times for one minute at RT; and (*8*) 2% glutaraldehyde for 10 minutes at RT. After washing with distilled water and drying, the sections were double stained with uranyl acetate and lead and then examined using an electron microscope. Control experiments were performed with the omission of the primary antibodies, but with the application of secondary antibodies.

In situ hybridization

In situ hybridization was performed by the method described in detail previously [22, 23], using cRNA probes generated from cDNA clones encoding rat α1(I) procollagen (generous gift from Y. Yamada, National Institutes of Health). Hybridization and the final wash were carried out at 55°C overnight with 2 × standard saline citrate (SSC) for 30 minutes at 50°C, respectively. Using these sections, DIF with anti-α-SMA and anti-VIM steps were carried out as described previously in this article.

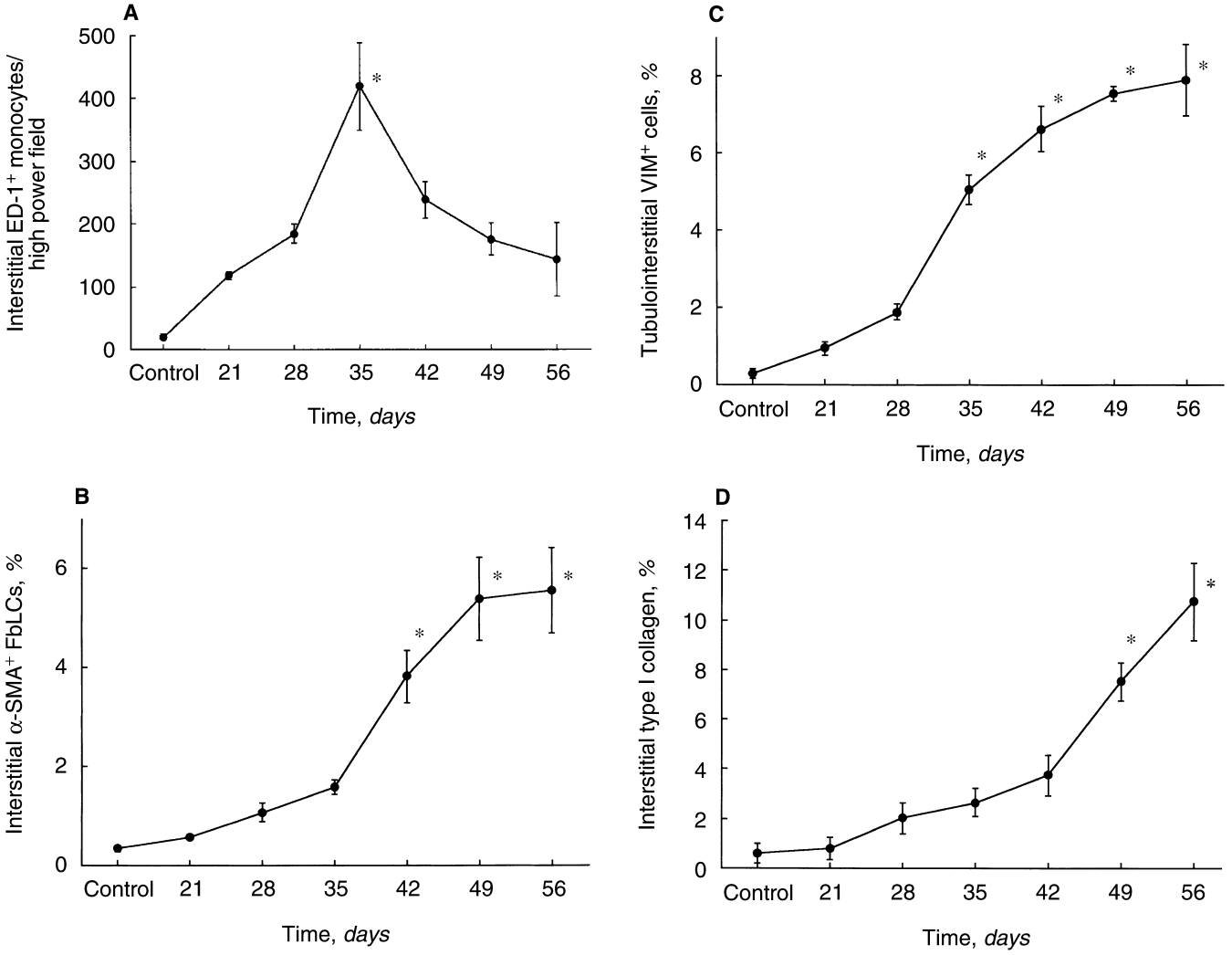

Fig. 1. Quantitative analysis of the morphological parameters in the renal cortex of Goodpasture syndrome (GPS) rats. (*A*) Interstitial infiltration of ED-1$^+$ monocytes. The number of ED-1$^+$ monocytes in the interstitium gradually increased, peaking at day 35, and then decreasing thereafter. (*B*) Interstitial α-smooth muscle actin$^+$ (α-SMA$^+$) fibroblast-like cells (FbLCs). The relative area of α-SMA$^+$ FbLCs in the interstitium gradually increased, peaking at day 49. (*C*) Tubulointerstitial vimentin$^+$ (VIM$^+$) cells. The relative area of VIM$^+$ tubular epithelium and interstitial FbLCs gradually increased until it reached a peak at day 49. (*D*) Interstitial accumulation of Col I. Finally, the relative area of Col I accumulation in GPS rats gradually increased in a time-dependent fashion and reached a peak at day 56. *$P < 0.05$.

RNase protection assay

Total RNA was extracted from the homogenates of whole kidneys with TRIzol™ (GIBCO BRL, Grand Island, NY, USA) according to the manufacturer's instructions. Ten micrograms of RNA were hybridized with ^{32}P-labeled antisense cRNA probes (1×10^5 counts/min) in combination with GAPDH antisense probes, synthesized by in vitro transcription using the linearized templates, at 45°C overnight. Unhybridized probes were digested with RNase A (0.3 mg/mL; Sigma) and RNase T1 (30 U/mL; GIBCO BRL) at 30°C for one hour. The cRNA probes were generated from cDNA fragments encoding rat α1(I) procollagen and rat TIMP-1 (generous gift from A. Okada, Tokyo University, Tokyo, Japan). The RNases were inactivated via proteinase K treatment at 37°C for 30 minutes. After phenol-chloroform extraction and ethanol precipitation had been performed, the hybridized probes protected from RNase digestion were denatured at 85°C for three minutes and electrophoresed on 6% polyacrylamide gels. The dried gels were exposed to x-ray films for 6 to 24 hours in order to detect signals. For quantifying each mRNA's expression, the autoradiograph bands were analyzed by computerized densitometry using Mac SCOPE. Data are presented as the ratio of specific mRNA to GAPDH mRNA (to equalize the quantity of RNA within each sample).

Statistical analysis

Values are presented as means ± SE. Statistical differences between the groups were evaluated by analyses of variance, followed by Duncan's multiple range test, with $P < 0.05$ used as the requirement for significance.

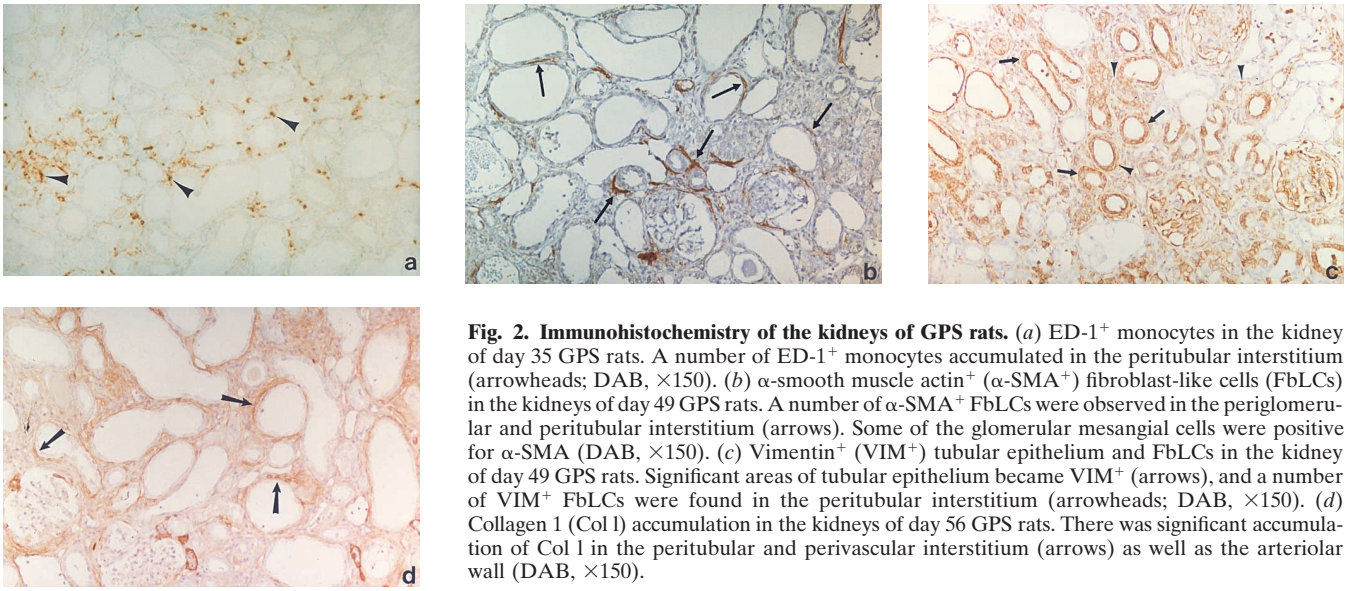

Fig. 2. Immunohistochemistry of the kidneys of GPS rats. (*a*) ED-1$^+$ monocytes in the kidney of day 35 GPS rats. A number of ED-1$^+$ monocytes accumulated in the peritubular interstitium (arrowheads; DAB, ×150). (*b*) α-smooth muscle actin$^+$ (α-SMA$^+$) fibroblast-like cells (FbLCs) in the kidneys of day 49 GPS rats. A number of α-SMA$^+$ FbLCs were observed in the periglomerular and peritubular interstitium (arrows). Some of the glomerular mesangial cells were positive for α-SMA (DAB, ×150). (*c*) Vimentin$^+$ (VIM$^+$) tubular epithelium and FbLCs in the kidney of day 49 GPS rats. Significant areas of tubular epithelium became VIM$^+$ (arrows), and a number of VIM$^+$ FbLCs were found in the peritubular interstitium (arrowheads; DAB, ×150). (*d*) Collagen 1 (Col l) accumulation in the kidneys of day 56 GPS rats. There was significant accumulation of Col l in the peritubular and perivascular interstitium (arrows) as well as the arteriolar wall (DAB, ×150).

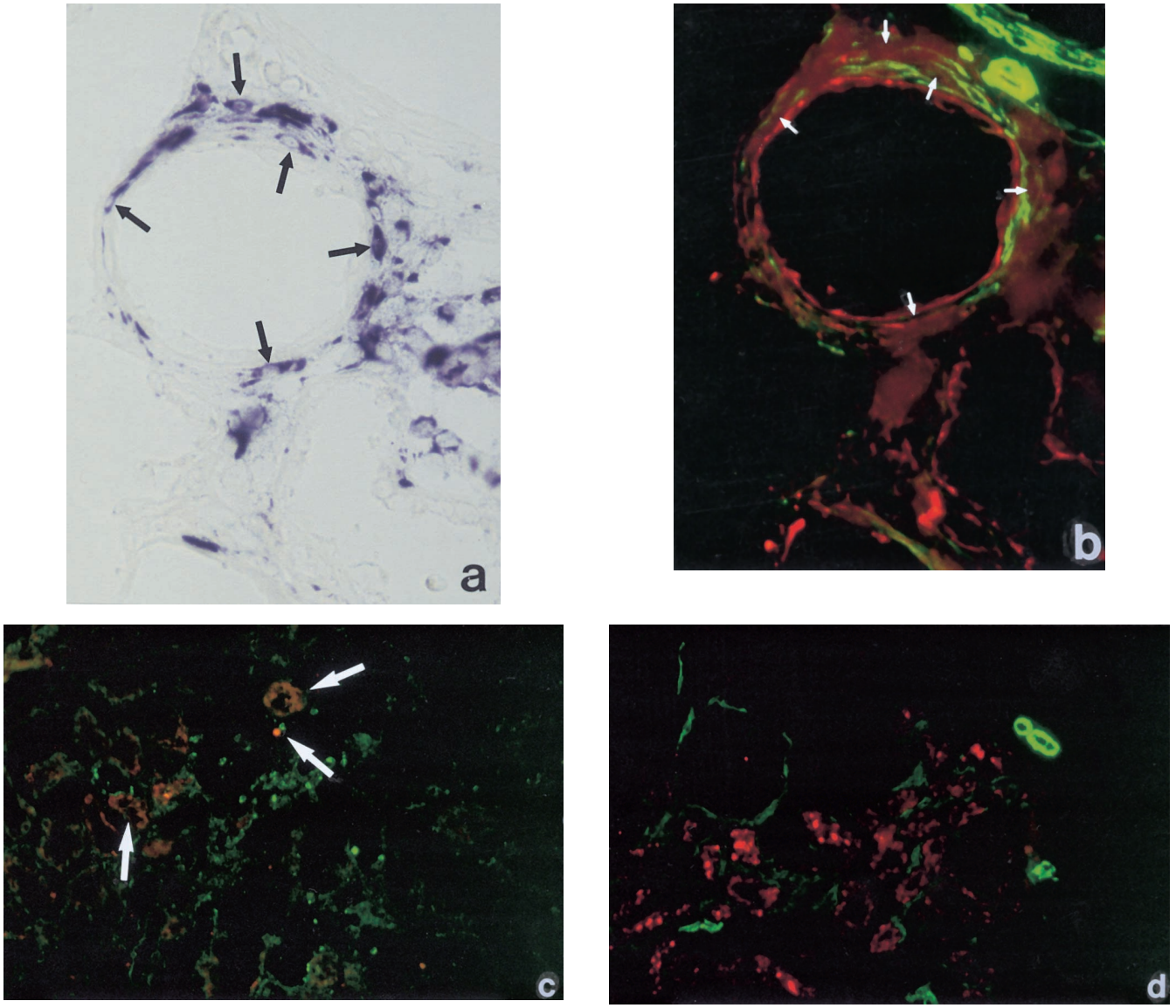

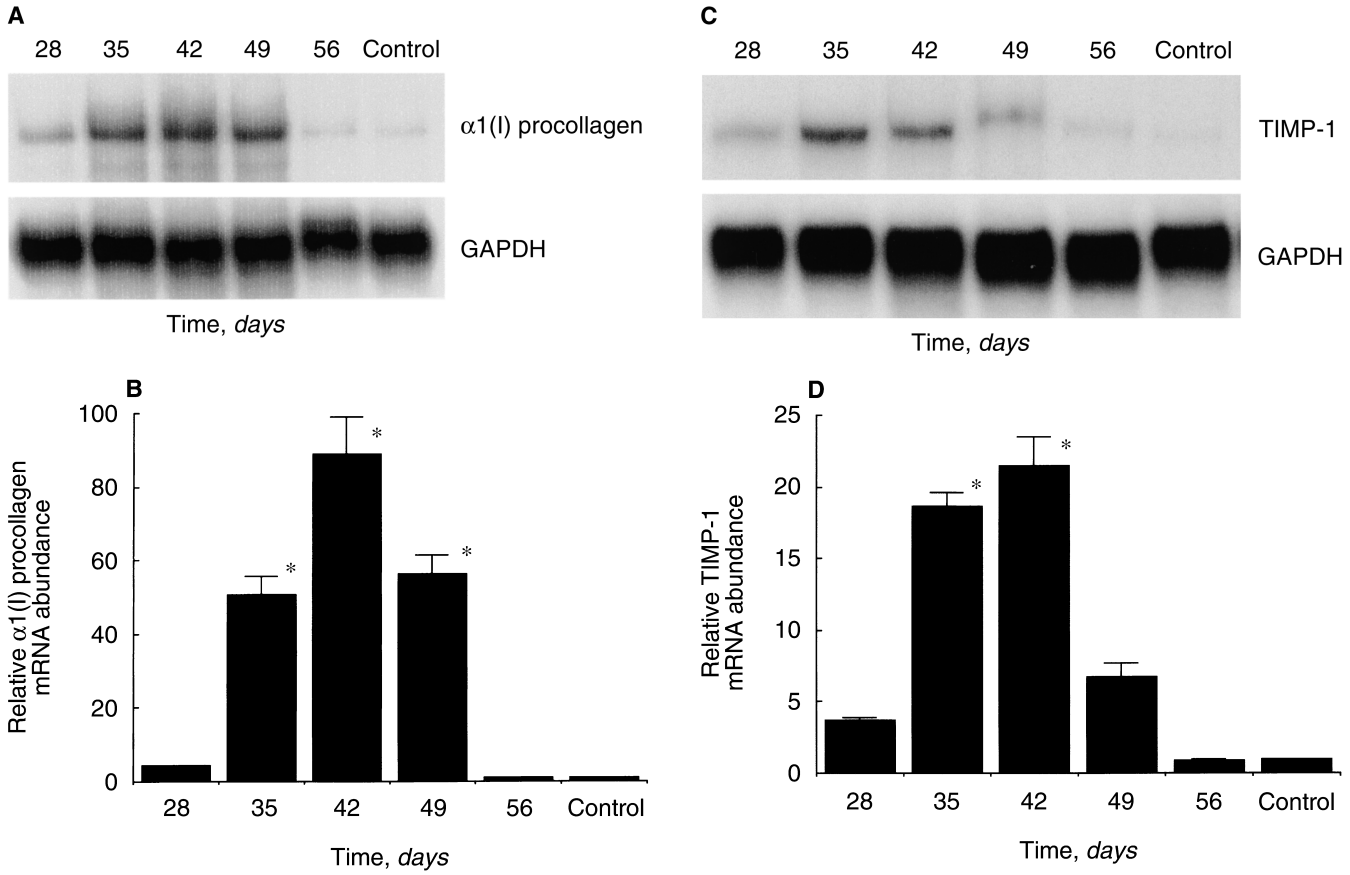

Fig. 3. RNase protection assay (RPA of the kidneys of GPS rats. (*A*) Expression of α1(I) procollagen mRNA. (*B*) Quantitative densitometric analysis of (A). Expression of α1(I) procollagen mRNA gradually increased to a peak around day 42 to 49 and then decreased (*$P < 0.05$). (*C*) Expression of TIMP-1 mRNA. (*D*) Quantitative densitometric analysis of (C). Expression of TIMP-1 mRNA gradually increased until it reached a peak around day 35 to 42 and then gradually decreased (*$P < 0.05$). Each blot is representative of three independent experiments, and the densitometric data were obtained from these three blots.

RESULTS

Characterization of renal interstitial fibrosis in GPS rats

As shown in Figure 1, the peak of interstitial infiltration by monocytes at day 35 preceded the increases in the number of α-SMA$^+$ FbLCs, the amount of VIM$^+$ tubular epithelium, and the number of VIM$^+$ FbLCs at approximately day 42 to 49 (Fig. 2 a–c). Thereafter, accumulation of Col I became significant in the interstitium of the renal cortex of GPS rats at day 56 (Fig. 2d). The expression of α1(I) procollagen mRNA was increased in a time-dependent fashion until it reached a peak around day 42 to 49 (Fig. 3 a, b), which preceded the prominent renal fibrosis with peak accumulation of Col I protein at day 56 (Fig. 1d). In Figure 2d, it can be seen that some of the arteriolar wall was positive for Col l. This implies that vascular smooth muscle cells produce increased levels of Col l in the nephritic kidney [24]. Similarly, the expression of TIMP-1 mRNA increased until it reached a peak around day 35 to day 42 (Fig. 3 c, d), possibly contributing to enhanced accumulation of interstitial collagens in GPS rats. From day 56, the GPS rats began to die, most likely from end-stage renal failure.

Fig. 5. Type I collagen- and TIMP-1-producing FbLCs in the kidneys of 49-day GPS rats. (*a*) In situ hybridization (ISH) for α1(I) procollagen mRNA. (BCIP/NT, ×400). (*b*) Dual immunofluorescence (DIF) for α-SMA (in green) and VIM (in red) on the same section of (a) (FITC and rhodamine, ×400). Peritubular FbLCs producing α1(I) procollagen (arrows) in Figure 5a were negative for α-SMA and VIM in (b). (*c*) TIMP-1 (in red) and VIM (in green). Most of the VIM$^+$ tubular epithelium and some of the VIM$^+$ FbLCs were simultaneously positive for TIMP-1, yielding yellow color (arrows). (FITC and rhodamine, ×200). (*d*) TIMP-1 (in red) and α-SMA (in green). α-SMA$^+$ FbLCs in green were negative for TIMP-1, shown in red (FITC & Rhodamine, ×200).

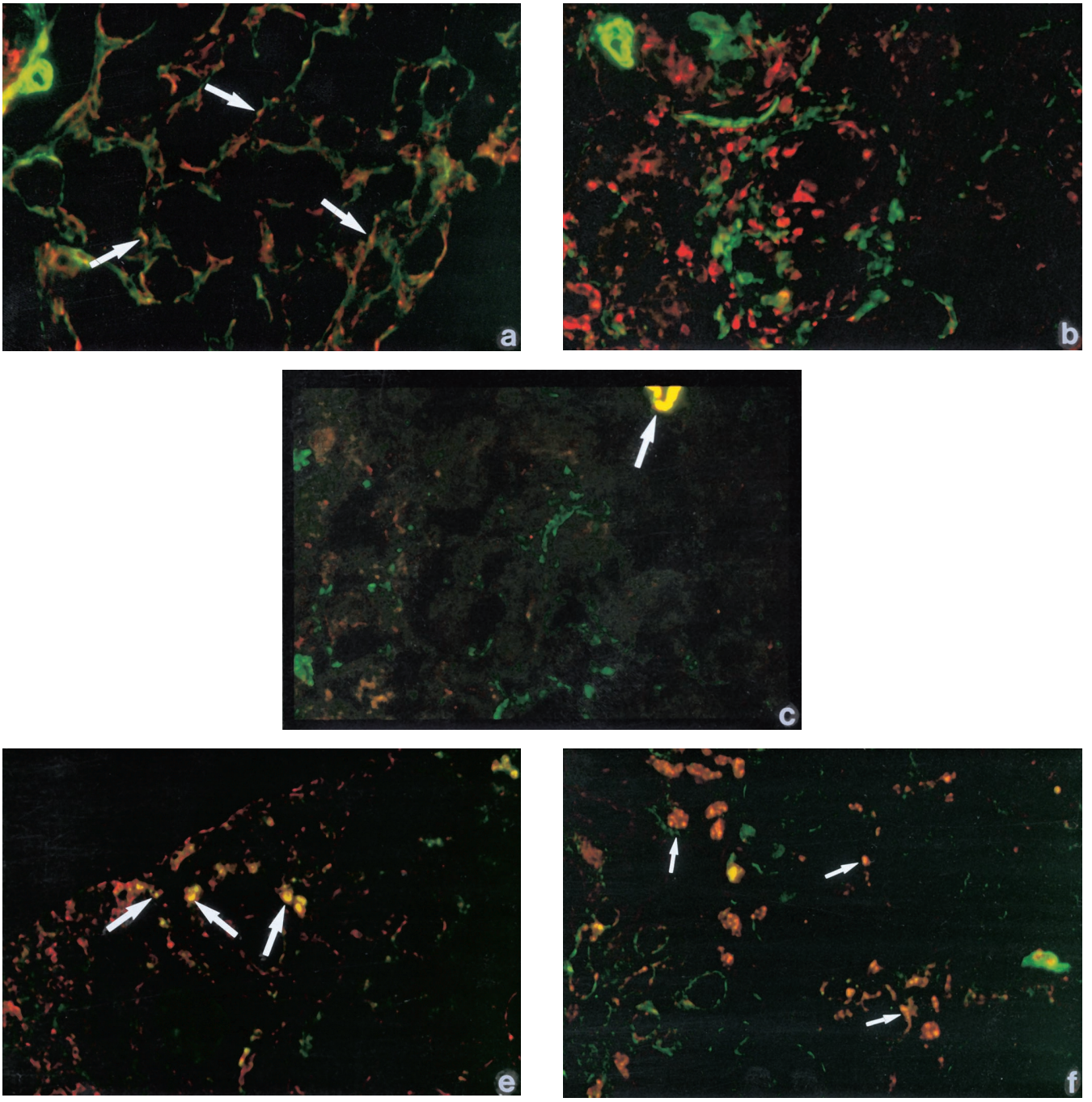

Fig. 4. Phenotypic/functional marker expression in interstitial FbLCs in the renal cortex of day 49 GPS rats. (*a*) α-Smooth muscle actin (α-SMA) (in green) and desmin (DSM) (in red). Most of the α-SMA$^+$ FbLCs in green were simultaneously positive for DSM in red, resulting in a number of FbLCs that ultimately appeared yellow (arrows; FITC and rhodamine, ×400). (*b*) α-SMA (in green) and VIM (in red). They were clearly different from each other, since there were no cells in yellow, indicating no dual-positive FbLCs (FITC and rhodamine, ×400). (*c*) α-SMA (in green) and myosin heavy chain (MYS) (in red). There were no MYS$^+$ FbLCs in red in the interstitium, and only vascular wall cells were doubly positive for α-SMA and MYS (arrow; FITC and rhodamine, ×400). (*d*) Immunoelectron microscopic observation of α-SMA$^+$ FbLCs. α-SMA$^+$ FbLCs were observed in the peritubular interstitium of the renal cortex. α-SMA$^+$ microfilaments (arrows) distributed in the perimembranous cytoplasm. There were no well-developed rough endoplasmic reticulum (rER) and actin-stress fibers within those cells (15 nm gold particle, ×4000). (*e*) TGF-β1 (in green) and VIM (in red). Some of the VIM$^+$ tubular epithelium and the VIM$^+$ FbLCs were simultaneously positive for TGF-β1, yielding yellow color (arrows; FITC and rhodamine, ×200). (*f*) PDGF-B chain (in red) and VIM (in green). Some tubular epithelium are shown in yellow (arrows), suggesting that some of the VIM$^+$ tubular epithelium were positive for both PDGF-B chain and VIM (FITC and rhodamine, ×200).

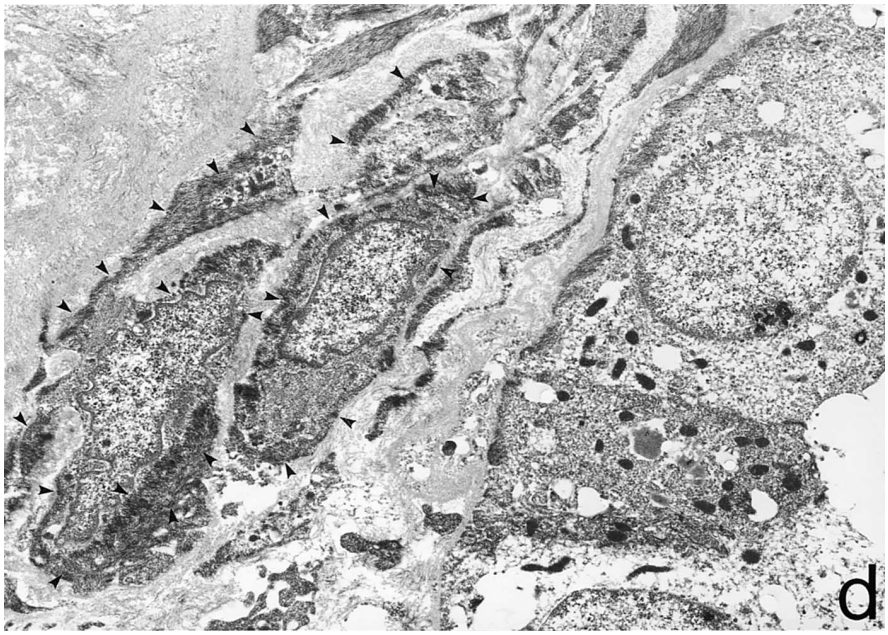

Fig. 4 (Continued).

Table 1. Dual immunofluorescence analysis of phenotypic markers

	α-SMA	VIM	DSM	MYS	TGF-β1	PDGF-B
α-SMA		VWCs[a]	FbLCs VWCs	VWCs	(−)	(−)
VIM			VWCs[a]	VWCs[a]	TECs FbLCs[a]	TECs[a]
DSM				VWCs	(−)	(−)
MYS					(−)	(−)
TGF-β1						NC
PDGF-B						

Abbreviations are: α-SMA, α-smooth muscle actin; VIM, vimentin; DSM, desmin; MYS, myosin heavy chain; TGF-β1, transforming growth factor-β1; PDGF-B, platelet-derived growth factor B chain; FbLCs, interstitial fibroblast-like cells; TECs, tubular epithelial cells; VWCs, vascular wall cells; (−), no dual positive cells; NC, not checked.

[a] Positive in occasional cells

Characterization of interstitial FbLCs in the nephritic kidney

Phenotypic marker expression. Given that day 49 GPS rats demonstrated significantly elevated numbers of α-SMA$^+$ and VIM$^+$ FbLCs and maximal expression of α1(I) procollagen mRNA, renal tissues of day 49 GPS rats were selected and evaluated in detail. Table 1 summarizes the phenotypic marker expression of interstitial FbLCs in the renal cortex of day 49 GPS rats. There were a number of α-SMA$^+$ FbLCs, most of which were simultaneously positive for DSM (Fig. 4a). Most of the VIM$^+$ FbLCs were negative for the other mesenchymal markers examined, including α-SMA (Fig. 4b). MYS expression was not seen in any interstitial FbLCs, but within the vascular wall cells (Fig. 4c). The expression of 5′-NT was not seen in any interstitial FbLCs (data not shown), suggesting abnormal intrarenal hemodynamics and erythropoietin synthesis [7]. In addition, no interstitial FbLCs, but some glomerular cells, were positive for PCNA in the kidney of day 49 GPS rats (data not shown), suggesting that FbLCs were productive but not proliferative around day 49 in this model.

Microstructure. Immunoelectron microscopy (IEM) revealed that the rough endoplasmic reticulum (rER) and actin stress-fibers were not well developed in the α-SMA$^+$ FbLCs within the renal cortex (Fig. 4d), which was clearly in contrast to typical myoFbs observed in the skin granulation tissue [9, 10].

Para/autocrine function. A summary of cytokine secretion by FbLCs is also shown in Table 1. TGF-β1 is positive in some VIM$^+$ tubular epithelium and VIM$^+$ FbLCs (Fig. 4e). In addition, PDGF-B chains were also present in some VIM$^+$ tubular epithelium (Fig. 4f).

Extracellular matrix metabolism. RNase protection assay (RPA) revealed that α1(I) procollagen mRNA was significantly expressed in the kidneys of day 49 GPS rats (Fig. 3 a, b). However, ISH/DIF demonstrated that neither α-SMA$^+$ nor VIM$^+$ FbLCs predominantly expressed α1(I) procollagen mRNA in those nephritic kidneys (Fig. 5 a, b), and therefore, the principle FbLCs responsible for Col I production remains unidentified. TIMP-1 gene expression was also found in the kidneys of those GPS rats (Fig. 3 c, d), and TIMP-1 protein was positive in some of the VIM$^+$ tubular epithelium and FbLCs, but was negative in the α-SMA$^+$ FbLCs (Fig. 5 c, d).

DISCUSSION

This study found that α-SMA$^+$ FbLCs are unlikely to be involved in Col I synthesis; however, we were not

able to determine which type of FbLCs were responsible for it. In contrast, based on the colocalization results, VIM$^+$ FbLCs were demonstrated to produce TGF-β1 and TIMP-1, and thus indirectly contribute to renal fibrogenesis. Recently, a growing number of nephrologists have become interested in renal fibrosis, given that the extent of renal fibrosis is the best predictor of functional prognosis [5, 6]. Via various elegant studies concerning myoFbs in skin granulation tissues, in which VIM$^+$/α-SMA$^+$ (VA-type) myoFbs with well-developed rER and actin-stress fibers have been demonstrated to synthesize interstitial ECM molecules and TGF-β1, and to retract surrounding tissues [9, 10, 25–28], all α-SMA$^+$ FbLCs residing within fibrotic areas of different organs have been presumed to engage in these same activities. Thus, renal α-SMA$^+$ FbLCs also have been thought to play an essential role in renal fibrosis in the same scenario [1–4, 29]. However, such α-SMA$^+$ FbLCs, presumed to be renal myoFbs, have never been characterized in detail. There have been a few studies investigating Col I-producing FbLCs in the kidney. In those studies, perivascular adventitial cells in anti-GBM nephritis [30], and peritubular interstitial cells in acute puromycin aminonucleoside nephrosis [31] and obstructive nephropathy [32] were found to produce Col I. However, the phenotypes of those cells were not determined. In contrast to liver, lung, and pancreas fibrosis, where α-SMA$^+$ FbLCs were confirmed to produce Col I [33–35], we demonstrated in this study that α-SMA$^+$ FbLCs were unlikely to act as the main producers of Col I in the kidney, at least during the peak of the fibrogenesis process in the kidneys of GPS rats. Less active Col I production by those renal interstitial α-SMA$^+$ FbLCs was consistent with the findings by IEM that they were not equipped with well-developed rER. In addition, most of these α-SMA$^+$ FbLCs were found to be negative for bundles of actin-stress fibers and TGF-β1, and to bear intermediate filaments of DSM instead of VIM in this study, all of which are apparent differences between renal α-SMA$^+$ FbLCs and granulation tissue myoFbs [9, 10]. Therefore, we should reconsider whether renal interstitial α-SMA$^+$ FbLCs are true myoFbs according to their original definition [9, 10]. Nevertheless, a contribution of those α-SMA$^+$ FbLCs to renal fibrogenesis cannot be excluded because some of them were positive for HSP47, a collagen-binding chaperone [36, 37], suggesting their involvement in collagen synthesis, and some were also found to produce Col III [19, 20]. In fact, the presence of α-SMA$^+$ FbLCs in the interstitium was reported to correlate with renal fibrosis and the worsening of renal function in several renal diseases, that is, IgA nephropathy [38] and diabetic nephropathy [39]. However, in contrast, Morrissey and Klahr recently reported that a decrease in the number of α-SMA$^+$ FbLCs in the renal interstitium resulted from angiotensin type 2 receptor blockade in rat obstructive nephropathy despite the progression of renal fibrosis [40]. Further studies are needed in order to prove their direct contribution to fibrogenesis in the nephritic kidney.

Either Col I or α-SMA colocalizes in granulation tissue myoFbs [9, 10], but not in renal FbLCs (Figs. 5 a, b). No common sequence indicating the putative FbLC-specific enhancer element was identified between the 5′ flanking regions of the α1(I) procollagen [41, 42] and α-SMA genes [43, 44]. Okada et al found a *cis*-acting element for FbLC-specific transcription of Fb-specific protein-1 (FSP1) that had been cloned as a murine FbLC-specific protein and named this element the Fb transcription site-1 (FTS-1) [45]. A search of the genomic database with the FTS-1 sequence identified identical sites in the early promoter regions of the α1(I) procollagen and α-SMA genes [45], which implies that both of them can be expressed in FSP1$^+$ FbLCs. However, distributions of FSP1 and α-SMA in some murine models of renal disease were clearly different [36], and those of Col I and α-SMA in GPS rat kidney also were found to be different in this study. Thus, FTS-1 seems unlikely to be strong enough alone in the promoter region of a given gene to govern its expression in a discrete type of FbLCs.

In the normal kidney, VIM$^+$ FbLCs have been traditionally recognized as typical Fbs similar to dermal VIM$^+$ FbLCs [8, 10]. In the case of a diseased kidney, we found that the renal interstitial VIM$^+$ FbLCs produced not Col I but TGF-β1 and TIMP-1, promoting renal fibrogenesis. These findings are compatible with the findings by Yamamoto, Noble and Border that sustained expression of TGF-β1 by the VIM$^+$ FbLCs underlies the development of renal fibrosis in the progressive form of anti–Thy-1 nephritis in rats [21]. As further supporting evidence, Isaka et al reported their success in transfection of TGF-β1 antisense oligodeoxynucleotides into renal interstitial FbLCs, which were likely to be VIM$^+$, and blocking the progression of renal fibrosis in rat obstructive nephropathy [46].

As indicated in the literature, VIM positivity in renal tubular epithelium is a feature of regeneration and the renal tubular epithelium is thought to control, at least partially, the phenotype of FbLCs and play an important role in renal fibrosis [2–4, 47–49]. Previously, we reported that tubular epithelium produced chemoattractants for monocytes (for example, monocyte chemoattractant protein-1 and osteopontin) that enrolled monocytes into the peritubular interstitium in GPS rats, giving rise to the early interstitial alterations seen prior to renal fibrosis [22, 23]. In addition to such chemoattractants, fibrogenic cytokines, for example, TGF-β1 and PDGF-BB, and TIMP-1 were produced exclusively by the tubular epithelium in this model, contributing to renal fibrogenesis. In fact, TIMP-1 mRNA expression in the nephritic kidney increased prior to the increase in α1(I) procollagen mRNA in this model, possibly accelerating collagen de-

position. This may be of greater importance than previously believed, since decreased collagen degradation is thought to be the most significant metabolic abnormality in some renal fibrosis models [2, 50].

We demonstrated that the interstitium in nephritic kidney contained a variety of FbLCs bearing functionally different phenotypes. In his excellent review article, Komuro proposed that a given organ's interstitium contains a complex network of highly differentiated FbLCs derived from different origins or common ancestor stem cells, and that each type of FbLC has its own functional contribution, that is, skin Fbs as ECM-producing FbLCs, and granulation tissue myoFbs as contractile and ECM-producing FbLCs [8]. According to his proposal and our findings, the renal interstitial α-SMA$^+$ FbLCs seem to be FbLCs the functions of which remain undetermined, and the VIM$^+$ FbLCs, which seem to be cytokine-secreting FbLCs. In addition, other FbLCs not characterized with the phenotypic markers used in this study are likely to be Col I-producing FbLCs. It seems feasible that native FbLCs, which are comprised of heterogeneous populations [25], vascular smooth muscle cells, vascular pericytes, and tubular epithelium [14], are differentiated or transformed into a variety of FbLCs in response to the environmental factors existing in the nephritic kidney.

In conclusion, our study reveals that the composition of the renal interstitium of GPS rats is far from simplistic, and suggests that the α-SMA$^+$ FbLCs directly contribute less to renal fibrogenesis than once believed. Renal fibrosis is a final common pathway leading to ESRD so that it may represent a common therapeutic target for a variety of progressive renal diseases. To establish a specific therapy against renal fibrosis, a key FbLC that orchestrates the rest of the FbLCs to promote the fibrogenesis is yet to be identified.

ACKNOWLEDGMENTS

The authors thank S. Yamada, J. Takahashi, and K. Tanaka for their technical assistance. Parts of this study were presented at the 30th and the 33rd Annual Meeting of the American Society of Nephrology, San Antonio, Texas, USA, November 2-5, 1997, and Toronto, Ontario, Canada, October 10–16, 2000. This study was previously partially published in abstract form (*J Am Soc Nephrol* 8:523, 1997, and 11:535, 2000).

Reprint requests to Hiromichi Suzuki, M.D., Ph.D., Department of Nephrology, Saitama Medical College, 38 Morohongo, Moroyama-machi, Irumagun, Saitama 350-04, Japan.
E-mail: iromichi@saitama-med.ac.jp

APPENDIX

Abbreviations used in this article are: α--SMA, α-smooth muscle actin; Col, collagen; DIF, dual immunofluorescence; DSM, desmin; ECM, extracellular matrix; ESRD, end-stage renal disease; Fbs, fibroblasts; FbLCs, fibroblast-like cells; FSP-1, Fb-specific protein 1; FTS-1, Fb transcription site-1; GBM, glomerular basement membrane; GPS, Goodpasture syndrome; HE, hematoxylin and eosin (stain); ISN, in situ hybridization; myoFbs, myofibroblasts; MYS, myosin heavy chain; PBS, phosphate-buffered saline; PCNA, proliferating cell nuclear antigen; PDGF, platelet-derived growth factor; rER, rough endoplasmic reticulum; RPA, RNase protection assay; RT, room temperature; TGF-β, transforming growth factor-β; TIMP-1, tissue inhibitor of metalloproteinase-1; VIM, vimentin.

REFERENCES

1. El Nahas AM, Muchaneta-Kubara EC, Essawy M, Soylemezoglu O: Renal fibrosis: Insights into pathogenesis and treatment. *Int J Biochem Cell Biol* 29:55–62, 1997
2. Eddy AA: Molecular insights into renal interstitial fibrosis. *J Am Soc Nephrol* 7:2495–2508, 1996
3. Okada H, Strutz F, Danoff TM, *et al*: Possible mechanisms of renal fibrosis. *Contrib Nephrol* 118:147–154, 1996
4. Remuzzi G, Ruggenenti P, Benigni A: Understanding the nature of renal disease progression. *Kidney Int* 51:2–15, 1997
5. Bohle A, Mackensen-Haen S, Von Gise H: Significance of tubulointerstitial changes in the renal cortex for the excretory function and concentration ability of the kidney: A morphometric contribution. *Am J Nephrol* 7:421–433, 1989
6. Striker G, Schainuck L, Cutler R, Beneditt E: Structural-functional correlations in renal disease. I. The correlations. *Hum Pathol* 1:615–630, 1970
7. Kaissling B, Hegyi I, Loffing J, Le Hir M: Morphology of interstitial cells in the healthy kidney. *Anat Embryol* 193:303–318, 1996
8. Komuro T: Re-evaluation of fibroblasts and fibroblast-like cells. *Anat Embryol* 182:103–112, 1990
9. Schmitt-Graeff A, Desmouliere A, Gabbiani G: Heterogeneity of myofibroblast phenotypic features: An example of fibroblastic cell plasticity. *Virchows Archiv* 425:3–24, 1994
10. Sappino AP, Schuerch W, Gabbiani G: Biology of disease: Differentiation repertoire of fibroblastic cells: Expression of cytoskeletal proteins as marker of phenotypic modulations. *Lab Invest* 63:144–161, 1990
11. Verbeek MM, Otte-Hoeller I, Wesseling P, *et al*: Induction of α-smooth muscle actin expression in cultured human brain pericytes by transforming growth factor-β1. *Am J Pathol* 144:372–382, 1994
12. Ronnov-Jessen L, Petersen OW, Koteliansky VE, Bissell MJ: The origin of the myofibroblasts in breast cancer. *J Clin Invest* 95:859–873, 1995
13. Powell DW, Mifflin RC, Valentich JD, *et al*: Myofibroblasts. I. Paracrine cells important in health and disease. *Am J Physiol* 277:C1–C19, 1999
14. Okada H, Danoff TM, Kalluri R, Neilson EG: Early role of Fsp1 in epithelial-mesenchymal transformation. *Am J Physiol* 273:F563–F574, 1997
15. Ng YY, Huang TP, Yang WC, *et al*: Tubular epithelial-myofibroblast transdifferentiation in progressive tubulointerstitial fibrosis in 5/6 nephrectomized rats. *Kidney Int* 54:864–876, 1998
16. Masur SK, Dewal HS, Dinh TT, *et al*: Myofibroblasts differentiate from fibroblasts when plated at low density. *Proc Natl Acad Sci USA* 93:4219–4223, 1996
17. Grupp C, Lottermoser J, Cohen DI, *et al*: Transformation of rat inner medullary fibroblasts to myofibroblasts in vitro. *Kidney Int* 52:1279–1290, 1997
18. Diamond JR, van Goor H, Ding G, Engelmyer E: Myofibroblasts in experimental hydronephrosis. *Am J Pathol* 146:121–129, 1995
19. Hewitson TD, Wu HL, Becker GJ: Interstitial myofibroblasts in experimental renal infection and scarring. *Am J Nephrol* 15:411–417, 1995
20. Tang WW, Van GY, Qi M: Myofibroblast and α1(III) collagen expression in experimental tubulointerstitial nephritis. *Kidney Int* 51:926–931, 1997
21. Yamamoto T, Noble N, Miller D, Border W: Sustained expression of TGF-β1 underlies development of progressive kidney fibrosis. *Kidney Int* 45:916–927, 1994
22. Okada H, Moriwaki K, Kalluri R, *et al*: Osteopontin expressed by renal tubular epithelium mediates interstitial monocyte infiltration. *Am J Physiol* 278:F110–F121, 2000
23. Okada H, Moriwaki K, Kalluri R, *et al*: Inhibition of monocyte chemoattractant protein-1 expression in tubular epithelium attenu-

ates tubulointerstitial alteration in rat Goodpasture syndrome. *Kidney Int* 57:927–936, 2000
24. Ford C, Li S, Pickering J: Angiotensin II stimulates collagen synthesis in human vascular smooth muscle cells. Involvement of the AT(I) receptor, transforming growth factor-beta, and tyrosin phosphorylation. *Atherioscler Thromb Vasc Biol* 19:1843–1851, 1999
25. Desmouliere A, Rubbia-Brandt L, Abdiu A, *et al*: α-Smooth muscle actin is expressed in a subpopulation of cultured and cloned fibroblasts and is modulated by γ-interferon. *Exp Cell Res* 201:64–73, 1992
26. Desmouliere A, Geinoz A, Gabbiani F, Gabbiani G: Transforming growth factor-β1 induces α-smooth muscle actin expression in granulation tissue myofibroblasts and in quiescent and growing cultured fibroblasts. *J Cell Biol* 122:103–111, 1993
27. Desmouliere A: Factors influencing myofibroblast differentiation during wound healing and fibrosis. *Cell Biol Int* 19:471–476, 1995
28. Desmouliere A, Redard M, Darby I, Gabbiani G: Apoptosis mediates the decrease in cellularity during the transition between granulation tissue and scar. *Am J Pathol* 146:56–66, 1995
29. El Nahas AM, Muchaneta-Kubara EC, Zhang GZ, *et al*: Phenotypic modulation of renal cells during experimental and clinical renal scarring. *Kidney Int* 49(Suppl 54):S23–S27, 1996
30. Wiggins R, Goyal M, Merritt S, Killen PD: Vascular adventitial cell expression of collagen I messenger ribonucleic acid in antiglomerular basement membrane antibody-induced crescentic nephritis in the rabbit. *Lab Invest* 68:557–565, 1993
31. Jones C, Buch S, Post M, *et al*: Renal extracellular matrix accumulation in acute puromycin aminonucleoside nephrosis in rats. *Am J Pathol* 141:1381–1396, 1992
32. Sharma AK, Mauer SM, Kim Y, Michael AF: Interstitial fibrosis in obstructive nephropathy. *Kidney Int* 44:774–788, 1993
33. Hoegemann B, Gillessen A, Boecker W, *et al*: Myofibroblast-like cells produce mRNA for type I and III procollagens in chronic active hepatitis. *Scand J Gastroenterol* 28:591–594, 1993
34. Zhang K, Rekhter MD, Gordon D, Phan SH: Myofibroblasts and their role in lung collagen gene expression during pulmonary fibrosis. *Am J Pathol* 145:114–125, 1994
35. Neuschwander-Tetri BA, Bridle KR, Wells LD, *et al*: Repetitive acute pancreatic injury in the mouse induces procollagen α(I) expression colocalized to pancreatic stellate cells. *Lab Invest* 80:143–150, 2000
36. Okada H, Ban S, Nagao S, *et al*: Progressive renal fibrosis in murine polycystic kidney disease: An immunohistochemical observation. *Kidney Int* 58:587–597, 2000
37. Cheng M, Razzaque M, Nazneen A, Tabuchi T: Expression of the heat shock protein 47 in gentamicin-treated rat kidneys. *Int J Exp Pathol* 79:125–132, 1998
38. Goumenos DS, Brown CB, Shortland J, El Nahas AM: Myofibroblasts, predictors of progression of mesangial IgA nephropathy? *Nephrol Dial Transplant* 9:1418–1425, 1994
39. Essawy M, Soylemezoglu O, Muchaneta-Kubara EC, *et al*: Myofibroblasts and the progression of diabetic nephropathy. *Nephrol Dial Transplant* 12:43–50, 1997
40. Morrissey JJ, Klahr S: Effect of AT2 receptor blockade on the pathogenesis of renal fibrosis. *Am J Physiol* 276:F39–F45, 1999
41. Liska D, Reed M, Sage E, Bornstein P: Cell-specific expression of α1(I) collagen-hGH minigenes in transgenic mice. *J Cell Biol* 125:695–704, 1994
42. Rossert J, Eberspaecher H, De Crombrughe B: Separate cis-acting DNA elements of the mouse pro-α1(I) collagen promoter direct expression of reporter genes to different type I collagen-producing cells in transgenic mice. *J Cell Biol* 129:1421–1432, 1995
43. Shimizu RT, Blank RS, Jervis R, *et al*: The smooth muscle alpha-actin gene promoter is differentially regulated in smooth muscle versus non-smooth muscle cells. *J Biol Chem* 31:7631–7643, 1995
44. Min B, Foster DN, Strauch AR: The 5′-flanking region of the mouse vascular smooth muscle α-actin gene contains evolutionarily conserved sequence motifs within a functional promoter. *J Biol Chem* 265:16667–16675, 1990
45. Okada H, Danoff T, Fischer A, *et al*: Identification of a novel cis-acting element for fibroblast-specific transcription of the FSP1 gene. *Am J Physiol* 275:F306–F314, 1998
46. Isaka Y, Tsujie M, Ando Y, *et al*: Transforming growth factor-β1 antisense oligonucleotides block interstitial ureteral obstruction. *Kidney Int* 58:1885–1892, 2000
47. Grone H, Weber K, Grone E, *et al*: Coexpression of keratin and vimentin in damaged and regenerating tubular epithelia of the kidney. *Am J Pathol* 129:1–8, 1987
48. Johnson DW, Saunders HJ, Baxter RC, *et al*: Paracrine stimulation of human renal fibroblasts by proximal tubule cells. *Kidney Int* 54:747–757, 1998
49. Palmer BF: The renal tubule in the progression of chronic renal failure. *J Invest Med* 45:346–361, 1997
50. Gonzalez-Avila G, Vadillo-Ortega F, Perez-Tamayo R: Experimental diffuse interstitial renal fibrosis. *Lab Invest* 59:245–252, 1988